

# Versatile Probes for the Selective Detection of Vicinal-Dithiol-Containing Proteins: Design, Synthesis, and Application in Living Cells

Chusen Huang,<sup>[a, b]</sup> Qin Yin,<sup>[b]</sup> Jiangjiang Meng,<sup>[b]</sup> Weiping Zhu,<sup>\*,[a]</sup> Yi Yang,<sup>[b]</sup>  
Xuhong Qian,<sup>[a, b]</sup> and Yufang Xu<sup>\*,[a, b]</sup>

**Abstract:** Endogenous vicinal-dithiol-containing proteins (VDPs) that have two thiol groups close to each other in space play a significant importance in maintaining the cellular redox microenvironment. Approaches to identify VDPs mainly rely on monitoring the different concentration of monothiol and total thiol groups or on indirect labeling of vicinal thiols by using *p*-aminophenylarsenoxide (PAO). Our previous work has reported the direct labeling of VDPs with a highly selective re-

ceptor PAO analogue, which could realize fluorescence detection of VDPs directly in living cells. Herein, we developed a conjugated approach to expand detectable tags to nitrobenzoxadiazole (NBD), fluorescein, naphthalimide, and biotin for the synthesis of a series of probes. Different linkers

**Keywords:** conjugation • fluorescent probes • imaging agents • redox • vicinal dithiols

have also been introduced toward conjugation of VTA2 with these functional tags. These synthesized flexible probes with various features will offer new tools for the potential identification and visualization of vicinal dithiols existing in different regions of VDPs in living cells. These probes are convenient tools for proteomics studies of various disease-related VDPs and for the discovery of new drug targets.

## Introduction

The homeostasis of a cellular redox environment is one of the most important foundations of living systems. Among the important factors associated with redox homeostasis and signaling, protein thiols are especially attractive for their direct involvement of many biological processes through post translational modification.<sup>[1]</sup> As the reductive form of the protein thiols, vicinal-dithiol-containing proteins (VDPs) with two space-closed thiol groups have been responsible for many diseases such as cancer,<sup>[2]</sup> diabetes,<sup>[3]</sup> human immunodeficiency virus type 1 (HIV-1),<sup>[4]</sup> and neurodegeneration.<sup>[5]</sup> The development of specific probes to trap and identify VDPs in biological milieu is of significant value to the pertinent studies.<sup>[6]</sup>

On the basis that trivalent arsenicals can form high-affinity ring structures with vicinal dithiols, most approaches to identify VDPs mainly rely on monitoring the different concentration of monothiol and total thiol groups through selective labeling of vicinal thiols with *p*-aminophenylarsenoxide (PAO). After blocking monothiols, then vicinal dithiols were labeled with thiol alkylation agent after the removal of PAO.<sup>[7]</sup> Arsenite(III)-affinity chromatography,<sup>[8]</sup> biotinylated conjugates of PAO,<sup>[9]</sup> and dimaleimide fluorogens<sup>[10]</sup> have also been developed to enrich and identify new VDPs and to make proteomic detection possible.<sup>[9,11]</sup> Despite these efforts, fluorescent and biotin-conjugated probes are still urgently needed to allow direct, noninvasive imaging of the dynamics of VDPs in living cells and unveil new VDPs with various functions that are closely related with different diseases. We have previously designed and conjugated highly selective receptor 2-*p*-aminophenyl-1,3,2-dithiarsenolane (VTA2) to naphthalimide, and realized the selective and direct detection of VDPs with fluorescence readout.<sup>[12]</sup> It is worthy to note that VTA2 is a stable, cell permeable, and selective ligand for VDPs.

Here we expanded the conjugated approaches to afford series of chemical probes through attachment of various detectable tags (naphthalimide, nitrobenzoxadiazole (NBD), fluorescein, and biotin) with different linkers (6-aminocaproic acid, succinic acid, and piperazine) to VTA2 (Figure 1). These probes with various properties will be used to identify the diversities of vicinal dithiols in VDPs in living cells<sup>[13]</sup> and present an alternative perspective for drug design.<sup>[13b]</sup> In particular, the fluorescence probes can enable the detection

[a] C. Huang, Prof. Dr. W. Zhu, Prof. Dr. X. Qian, Prof. Dr. Y. Xu  
Shanghai Key Laboratory of Chemical Biology, School of Pharmacy  
East China University of Science and Technology  
Meilong Road 130, Shanghai, 200237 (P.R. China)  
Fax: (+86) 21-64252603  
E-mail: wpzhu@ecust.edu.cn  
yfxu@ecust.edu.cn

[b] C. Huang, Q. Yin, J. Meng, Prof. Dr. Y. Yang, Prof. Dr. X. Qian,  
Prof. Dr. Y. Xu  
State Key Laboratory of Bioreactor Engineering, School of Pharmacy  
East China University of Science and Technology  
Meilong Road 130, Shanghai, 200237 (P.R. China)

Supporting information for this article is available on the WWW  
under <http://dx.doi.org/10.1002/chem.201300567>.

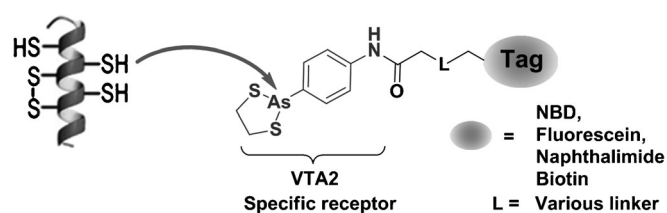


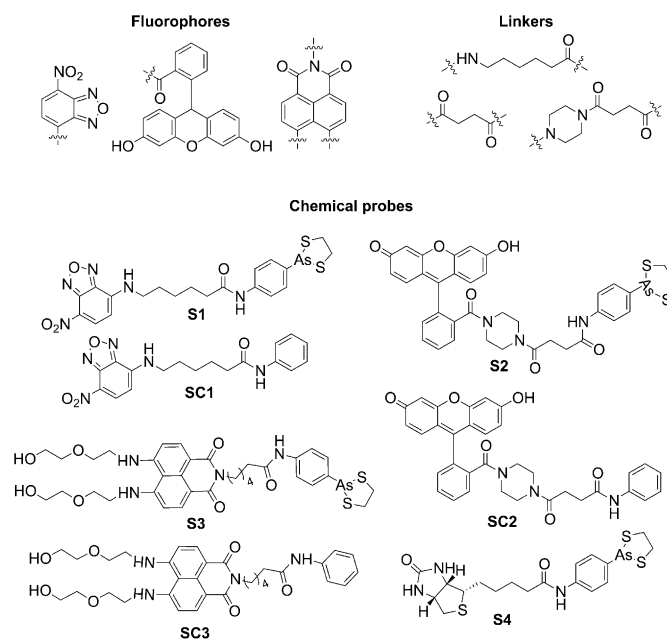
Figure 1. Design strategy of probes for direct detection of VDPs.

of VDPs with direct observation of fluorescence both on gel electrophoresis and in living cells.

## Results and Discussion

**Design strategy of probes for VDPs:** VDPs have received considerable attention in the past decade.<sup>[14]</sup> However, it is difficult to determine protein vicinal dithiols in situ due to the reversibility between vicinal dithiols and disulfides within living cells and during sample processing. An ideal detection method for protein vicinal dithiols should be rapid, specific, effective, and in situ, avoiding transfer or loss of the modification signal in the process. Since vicinal dithiol can form a stable, five-membered ring with **PAO**,<sup>[15]</sup> and monothiols of proteins have much lower affinity,<sup>[16]</sup> **PAO** has been widely used in its specific interaction with vicinal thiols on proteins. Most strategies have been implemented in the selective tracing of VDPs by using **PAO** to block vicinal dithiols following thiol alkylation agents to label other thiols. Finally, the vicinal dithiols were labeled after the removal of **PAO**.<sup>[7]</sup> To simultaneously monitor the VDPs and their dynamic response in living cells, especially the role of VDPs in the regulation of biological process, a fluorescent probe was a better choice since the detection signal of labeled-VDPs can be visualized directly.

In our previous report, we have developed the stable and specific vicinal dithiol ligand **VTA2**, which can selectively interact with vicinal thiols on proteins. By conjugation of the naphthalimide fluorophore with **VTA2** to form **S3** (Scheme 1), the endogenous VDPs can be visualized directly on SDS-PAGE and in living cells through the direct fluorescence readout. Herein, we now expand the conjugated strategies to afford probes with different properties for the direct labeling of endogenous VDPs utilizing various functional tags including NBD, fluorescein, and biotin (**S1**, **S2**, and **S4**, Scheme 1, for the detailed synthesis see the Supporting Information). Different linkers (6-aminocaproic acid, succinic acid, and piperazine) were also introduced for the conjugation of **VTA2** with these tags. For the identification and selective tracing of VDPs in living cells, the control probes (**SC3**, **SC1**, and **SC2**, Scheme 1, detailed synthetic procedures were described in the Supporting Information) without trivalent arsenical were also synthesized. **S4** was prepared for potential application in proteomic analysis of VDPs in cell lysis. A mechanism in which **S1**, **S2**, **S3**, and **S4** can selectively label VDPs through the specific interchange



Scheme 1. Molecular structures of target and control probes for VDPs.

of 1,2-ethanedithiol (EDT) in cyclic dithiaarsanes of probes with vicinal dithiols on proteins has been elucidated in detail.<sup>[12]</sup> The detailed synthetic design of probes and their potential application in the labeling of diversities of vicinal dithiols in various VDPs according to the different properties of probes are discussed in the following sections.

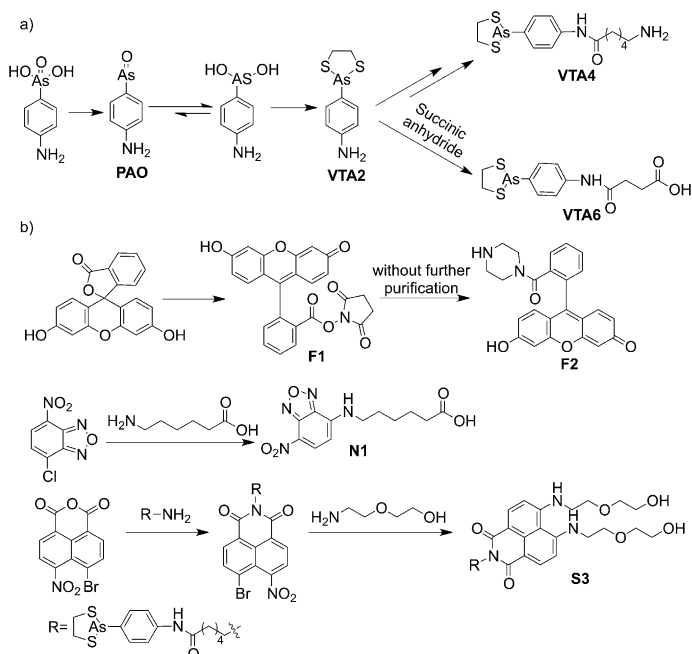
**Synthetic approaches for synthesis of probes for VDPs:** In our initial synthetic approaches, the starting material **PAO** was used directly to conjugate with different tags through various coupling reagents. However, **PAO** exists as hydrate,<sup>[17]</sup> which makes the purification of **PAO**-based derivatives difficult on a silica chromatographic column. Although **PAO** is a popular specific ligand for protein vicinal dithiols, it is easily oxidized<sup>[18]</sup> and no longer exists as a monomer over time,<sup>[17]</sup> which means the freshly synthesized **PAO** can only be used in one conjugation reaction. All these factors hinder the direct coupling reaction of **PAO** with tags and results in low product yields during the synthesis of target probes. Another major consideration was that **PAO** will lose the specific affinity for vicinal dithiols during oxidation of trivalent arsenic in **PAO** to pentavalent arsenic. The stable crystal structure of tolylarsenic 2,3-dimercaptopropanolate complex<sup>[15]</sup> and biarsenical fluorescent analogues<sup>[19]</sup> promoted us to explore a relatively facile synthetic strategy involving protection of **PAO** with 1,2-ethanedithiol (EDT) to first obtain the stable receptor **VTA2**. Next, different tags can then be conjugated with **VTA2**. Our previous report has revealed that **VTA2** was not only more stable but also a highly selective receptor for vicinal thiols in proteins. **VTA2** can selectively discriminate vicinal dithiols from other forms of thiols through the interchange of 1,2-ethanedithiol (EDT) in cyclic dithiaarsanes with vicinal dithiols in proteins.

Next, we explored the coupling reactions of **VTA2** with different tags through various linkers (Scheme 1). The biotinylated probe (**S4** in Scheme 1) was easily obtained in 72% yield through just one step by utilizing a classical coupling reagent *O*-(7-azabenzotriazol-1-yl)-*N,N,N',N'*-tetramethyluronium hexafluorophosphate (HATU, see the detailed information in Scheme S2 and the Supporting Information), which was better than the multistep methodology. This versatile coupling strategy was also involved in the conjugation of **VTA2** with NBD, 5(6)-fluorescein, and 1,8-naphthalic anhydride under various conditions in our previous effort (see the detailed synthetic route in Scheme S1, the Supporting Information). However, thin-layer chromatography (TLC) and NMR analyses showed no products were observed, which may be due to the more rigid structures of target probes just within NBD (fluorescein or 1,8-naphthalic anhydride) and **VTA2** (detailed molecular structures in Scheme S1, the Supporting Information). Another major factor that promotes us to introduce conjugated linkers was that the rigid structures of designed probes (structures in Scheme S1, the Supporting Information) may not enter into some target regions of VDPs and cannot interact with vicinal thiols effectively, which may cause a decrease in the labeling efficiency. Thus, different linkers were introduced to allow the efficient coupling of **VTA2** with various functional tags to afford different flexible probes. One strategy for accomplishing this involved two flexible linkers, 6-aminocaproic acid and succinic acid, which were introduced at the same amino site of **VTA2**. 6-aminocaproic acid can be easily conjugated to **VTA2** in three steps to form **VTA4** (Scheme 2).

Similarly, treatment of succinic anhydride with **VTA2** gave **VTA6** (Scheme 2) in nearly quantitative yield. These two flexible **VTA2** analogues with one free amino and carboxyl group, respectively, can be easily conjugated to various tags. The piperazine was conjugated to succinic acid to form the piperazine alkyl ether linker, which was another important linker because the nitro atoms of piperazine can form a hydrogen bond with amino acid in some region of the protein. Additionally, this piperazine moiety can give rigidity to the flexible linker and modulate the balance between the rigidity and the flexibility of the probe.<sup>[20]</sup>

An alternative approach was the development of derivatives of the fluorophores with sites that can be conveniently conjugated with **VTA2**. Fluorescein was first activated with *N*-hydroxysuccinimide (NHS). After the byproduct (dicyclohexylurea) was filtered off, the filtrate can be treated with anhydrous piperazine to directly synthesize **F2** (Scheme 2). This one-pot reaction can afford **F2** without further purification of the fluorescein-activated derivative (**F1**, Scheme 2) by using column chromatography and thus avoiding the instability of the active intermediate **F1** (see the detailed synthesis in the Supporting Information). By coupling NBD with 6-aminocaproic acid in basic conditions, the NBD derivative (**N1**, Scheme 2, see the detailed synthesis in the Supporting Information) was also obtained. The free amino group of **F2** (or free carboxyl of **N1**) can also aid the further conjugation of fluorescein (or NBD) with **VTA2** and its analogues conveniently. 1,8-Naphthalic anhydride was another derivative of the fluorophore with easy derivation. In our previous report, **VTA4** can be attached to the anhydride group in ethanol heated at reflux. Most importantly, different groups, such as biocompatible diglycol amine, poly(ethylene glycol), can be conveniently attached to the 4- and 5-positions of 1,8-naphthalimide, which will make the target probe more suitable for different applications in the biological milieu.

**The spectroscopic properties of S1, S2, and S3:** For the specific trapping of endogenous VDPs, the probe must be selective, stable, and biocompatible.<sup>[21]</sup> Our investigation began with analyzing the effect of pH on the UV/Vis and fluorescence spectra of **S1** and **S2**. As shown in Figure 2a, c, and e (detailed information in Figure S1, the Supporting Information), the intensity of the UV/Vis and fluorescence spectra of **S1**, **S2**, and **S3** was relatively stable at physiological conditions. Thus, phosphate-buffered saline (10 mM PBS, pH 7.4, 1% DMSO) was taken as the test solution in the following sodium dodecyl sulfate polyacrylamide gel electrophoresis (SDS-PAGE) and cell-imaging assay. **S1**, **S2**, and **S3** displayed suitable excitation and emission wavelength (495/553, 500/523, and 460/538 nm, respectively, Figure 2b, d, and f) in PBS buffer. These fluorescence properties of **S1**, **S2**, and **S3** enable them to label VDPs in living cells. Moreover, the fluorescence intensity of **S1**, **S2**, and **S3** changes at different pH values. **S1** can work in a broad pH range without a change of its fluorescence intensity. The suitable pH range for **S2** was above 7.4, whereas the fluorescence intensity of



Scheme 2. Approaches for synthesis of different probes for VDPs. a) Approaches for synthesis of **VTA2** and its analogues. b) An alternative approach for the synthesis of probes through derivatization of the fluorophore.

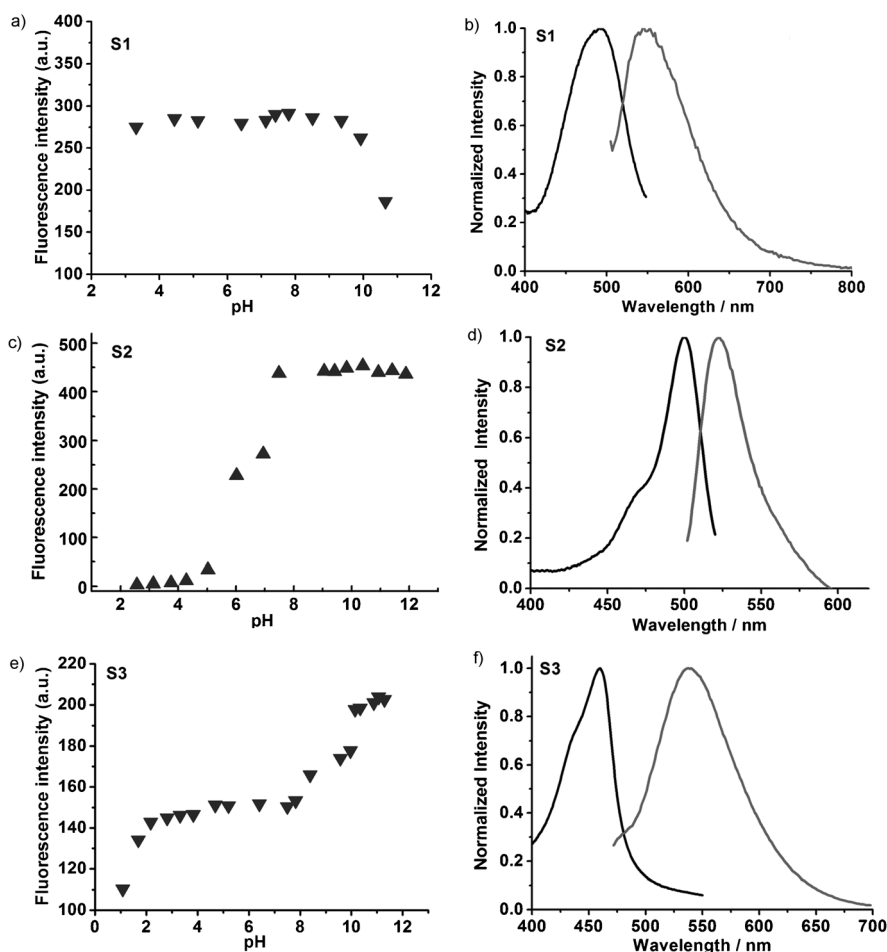


Figure 2. Influence of pH on the fluorescence intensity of a) **S1**, c) **S2**, and e) **S3** in water solution. Normalized absorption (left) and fluorescence spectra (right) of b) **S1**, d) **S2**, and f) **S3** in PBS buffer (10 mM PBS, pH 7.4, 1% DMSO).

**S3** remained stable at pH 5–8. All these fluorescence properties of the three probes make them suitable for labeling VDPs at a different pH range.

#### Selectivity of **S1** and **S2** for VDPs by using SDS-PAGE:

The specific assay of **S1** and **S2** for vicinal dithiols in proteins was conducted by SDS-PAGE. We used the reduced form of Trx (rTrx, see the detailed amino acid sequence in our reported literature<sup>[12]</sup>) as a typical VDP that only contains one pair of vicinal thiols. A mono-thiol mutant of thioredoxin (Trx-M, with C69G mutation) and oxidized thioredoxin (oTrx, the vicinal dithiol of oTrx was oxidized by H<sub>2</sub>O<sub>2</sub> immediately) were taken as the control model protein. These different forms of Trx were incubated with **S1** and **S2**, respectively, and then separated by electrophoresis. A fluorescent band was observed only in the lane loaded with rTrx and **S1** (or **S2**), whereas lanes loaded with oTrx or Trx-M exhibited no fluorescence signal (Figure 3). By contrast, these forms of Trx were observed on the subsequent Coomassie Brilliant Blue (CBB) staining, which demonstrated that the fluorescent band corresponded to the formation of a probe-

labeled rTrx (Figure 3). All these results indicated the high selectivity of **S1** (or **S2**) for vicinal dithiol in rTrx.

**MTT assay:** Next, to confirm the potential availability of **S1** and **S2** in the in situ imaging of VDPs, cytotoxicity assays were performed to evaluate the biocompatibility of these two probes. As shown by the Cell-Titer 96 AQueous non-radioactive cell proliferation assay, minimal cytotoxicity at the concentration of 0–25 μM was detected (Figure 4), suggesting the high biocompatibility of **S1** and **S2**. This result promoted our further investigation on live-cell labeling of endogenous VDPs by using this chemical probe-based fluorescent technology.

#### Discussion of the potential labeling of various VDPs with different probes in living cells:

Living cells are rich in VDPs, but the microenvironments that the VDPs exist in differ. Many VDPs are enzymes the active sites of which are vicinal thiols.<sup>[22]</sup> However, the active cores of these enzymes are dif-

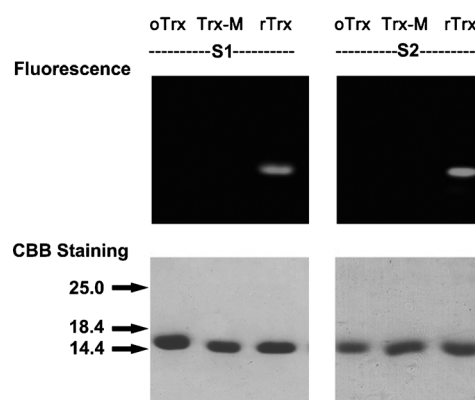


Figure 3. Fluorescent imaging of VDPs with **S1** and **S2** by using SDS-PAGE. oTrx: thioredoxin (Trx) oxidized immediately by hydrogen peroxide (H<sub>2</sub>O<sub>2</sub>); Trx-M: reduced thioredoxin mutation (Trx C69G); rTrx: reduced thioredoxin; CBB: Coomassie Brilliant Blue.

ferent according to their functional diversities, which indicates that the microenvironments of vicinal dithiols may

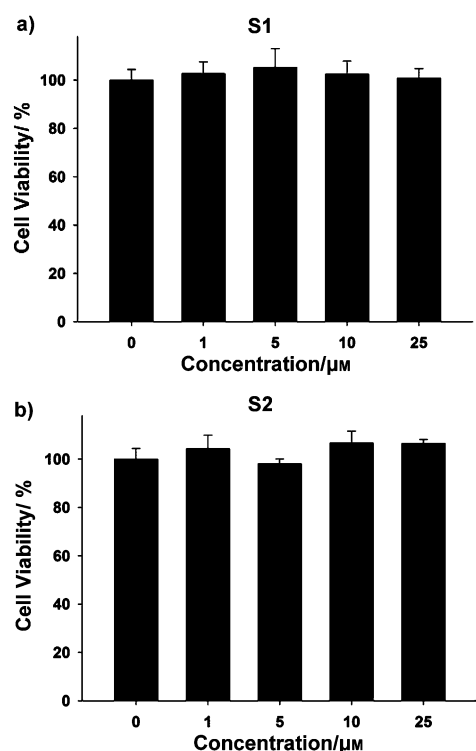


Figure 4. MTT assay for cell toxicity of **S1** and **S2**. Cell viability assay in the presence of different concentrations of a) **S1** and b) **S2**. The data were the average of quadruplicate measurements. Error bars:  $\pm$ S.E.M. The image was plotted according to the Promega CellTiter 96 AQueous non-radioactive cell proliferation assay.

differ between different types of VDPs and the nature of the microenvironments. Thus, the development of different probes for selective labeling of these different vicinal dithiols in the various enzymes was a great challenge. Here, we discuss the potential application of our probes in the labeling of these various vicinal dithiols in VDPs. The  $\log P$  values of target probes and their controls were estimated by using the shake-flask method. As shown in Figure 5a, probe **S1** was a more hydrophobic fluorescence probe compared with **S2** and **S3**, which makes it more cell-permeable and accessible to hydrophobic regions of VDPs. An interesting characteristic of **S1** (with NBD fluorophore) was its sensitivity to the environment.<sup>[23]</sup> The fluorescence quantum yield of **S1** increased from 0.02 to 0.30 after addition of 0.5% Tween to the PBS buffer (Table S1, detailed photoproperties of other probes are shown in Table S1 in the Supporting Information) because the surfactant Tween can form a hydrophobic microenvironment for **S1**. This was also identified by a small blue-shift in absorbance and significant increase in fluorescence intensity of **S1** with the addition of 0.5% Tween to PBS (Figure S2, the Supporting Information). The increase of fluorescence intensity of **S1** with decreasing polarity of the medium can make it suitable for labeling of vicinal dithiols existing in the hydrophobic regions of VDPs (such as the vicinal dithiol in hydrophobic core of glucosamine-6-phosphate deaminase).<sup>[24]</sup> Fluorescein is a cell-imper-

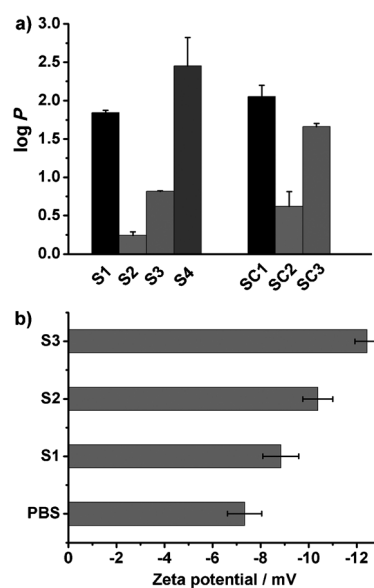


Figure 5. a) The  $\log P$  values of different probes (**S1**:  $1.84 \pm 0.03$ , **S2**:  $0.24 \pm 0.04$ , **S3**:  $0.81 \pm 0.01$ , **S4**:  $2.45 \pm 0.37$ ). b) Zeta potentials of different probes in PBS buffer (10 mM, pH 7.4, 1% DMSO). The data were the average of more than three measurements. Error bars:  $\pm$ S.E.M.

meable fluorophore at physiological conditions.<sup>[25]</sup> To realize the live-cell labeling of VDPs, the fluorescein was linked to **VTA2** through a relatively hydrophobic linker (piperazine alkyl ether linker, Scheme 1) to increase the cell-permeability of **S2**. Although the  $\log P$  value of **S2** was increased, its value was still relatively lower than other probes ( $0.24 \pm 0.04$ , Figure 5a). However, this increased hydrophilicity of **S2** makes it more prone to label vicinal dithiols in the hydrophilic region of VDPs relative to other probes. The mid-range  $\log P$  value of **S3** ( $0.81 \pm 0.03$ , in contrast to **S1** and **S2**, Figure 5a) may make it unbiased in the labeling of VDPs.

By comparing to the potential application in selective labeling of various VDPs depending on the hydrophobic (or hydrophilic) property of probes, the different electrostatic potentials of probes also can be utilized to trace VDPs with different isoelectric point (pI) in living cells. As shown in Figure 5b, different electrostatic potentials of these probes in PBS buffer can be observed. The lowest electrostatic potential of **S3** was ascribed to the attachment of two diglycolamine to the 4 and 5 positions of naphthalimide. This feature of **S3** may make it more prone to label VDPs with positive electrostatic potential in living cells. In addition, all the fluorescent probes with different electrostatic potentials may also be used to label various vicinal dithiols in VDPs with different isoelectric points (pI). In conclusion, diverse vicinal thiols in various VDPs may be labeled by these selective probes according to their different properties.

**Fluorescent labeling of VDPs in live cells:** Firstly, we performed the fluorescent labeling of endogenous VDPs in living cells using **S1**, **S2**, and **S3** through fluorescence microscopy. Chang liver cells were incubated with the probe for

30 min at 37°C and then washed to remove the free probe before the fluorescence signal was collected. As shown in Figure 6, cells treated with **S1** (or **S2**, **S3**) showed a strong

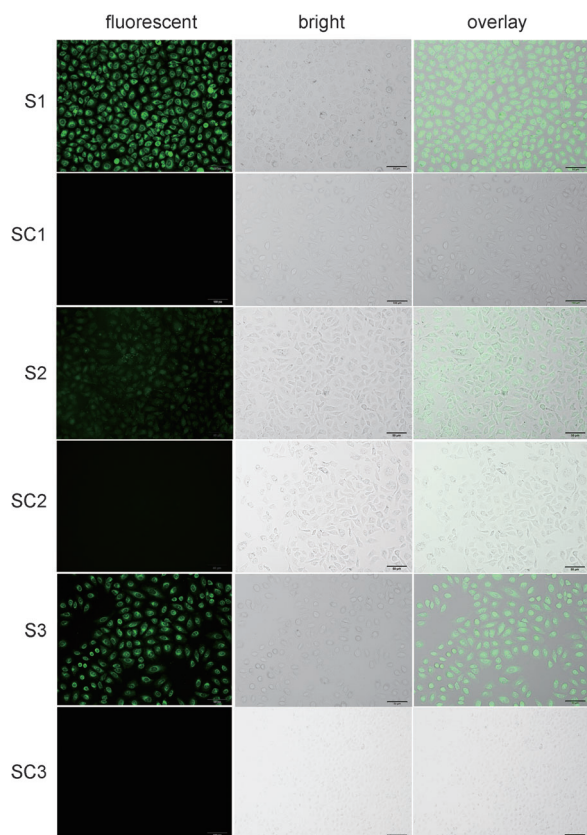


Figure 6. In situ imaging of VDPs in Chang liver cells. Fluorescent images of cells labeled with **S1** (5  $\mu\text{M}$ ; scale bar=50  $\mu\text{m}$ ), control probe **SC1** (5  $\mu\text{M}$ ; scale bar=100  $\mu\text{m}$ ), **S2** (5  $\mu\text{M}$ ; scale bar=50  $\mu\text{m}$ ), control probe **SC2** (5  $\mu\text{M}$ ; scale bar=50  $\mu\text{m}$ ), **S3** (5  $\mu\text{M}$ ; scale bar=50  $\mu\text{m}$ ), and control probe **SC3** (5  $\mu\text{M}$ ; scale bar=100  $\mu\text{m}$ ). Images were taken with an Olympus IX71 microscope equipped with a 20 $\times$  objective.

fluorescence signal. In contrast, only a background signal was observed from cells treated with the control probe (**SC1**, **SC2**, or **SC3**). These results suggested that **S1**, **S2**, and **S3** can be used in the selective labeling of endogenous VDPs in living cells, which was consistent with the SDS-PAGE results. These results also confirmed that the specific binding of **S1** (or **S2**, **S3**) to VDPs in living cells occurred through the interaction of vicinal thiols on VDPs with reactive cyclic dithiaarsanes in **S1**, **S2**, and **S3**.

It is interesting that the fluorescence intensity of **S2**-treated cells was lower than that of **S1**- (or **S3**)-treated cells under the same conditions. We ascribed this phenomenon to the low cell permeability of fluorescein at physiological condition.<sup>[25]</sup> After the fluorescein was linked to **VTA2** through a relatively hydrophobic piperazine alkyl ether linker (Scheme 1), the cell-permeability of **S2** might be increased (see the log *P* value in Figure 5a). This feature may enable **S2** to label intracellular VDPs in living cells. However, the

cell permeability of **S2** may be still relatively lower than **S1** (or **S3**), which will hinder the labeling efficiency of **S2** for endogenous VDPs in living cells. On the other hand, the hydrophilic characteristics of **S2** may make it more suitable for labeling of hydrophilic VDPs; this needs to be further investigated in our experiments.

Next, the application of **S3** for subcellular labeling VDPs was explored in Chang liver cells by using confocal microscopy. As shown in Figure 7a, the **S3** labeled fluorescence

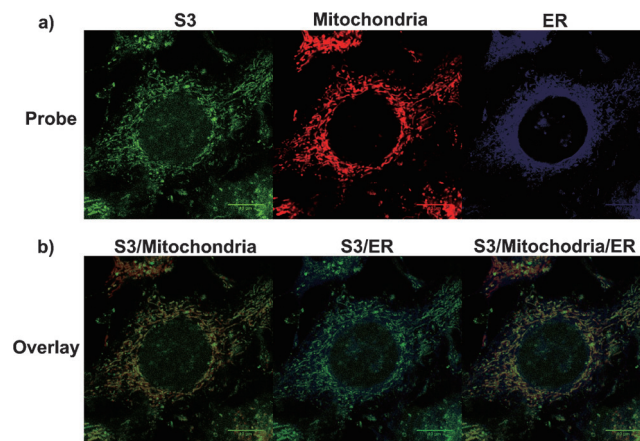


Figure 7. Application of **S3** for labeling subcellular VDPs in Chang liver cells. Triple staining of endoplasmic reticulum (ER), mitochondria and VDPs with ER-tracker Blue-White DPX, Mito-Tracker Deep Red and **S3** (5  $\mu\text{M}$ ). a) Fluorescence signal of **S3**, Mito-Tracker Deep Red and ER-tracker Blue-White DPX labeled, respectively. b) Co-localization of **S3** with Mito-Tracker Deep Red and ER-tracker Blue-White DPX. **S3**/Mitochondria: overlay image of **S3** and Mito-Tracker Deep Red; **S3**/ER: overlay image of **S3** and ER-tracker Blue-White DPX; **S3**/Mitochondria/ER: overlay image of **S3**, Mito-Tracker Deep Red and ER-tracker Blue-White DPX. Scale bar=10  $\mu\text{m}$ . Images were taken with an Olympus FV1000+IX481 confocal laser scanning microscopy by using UPLSAPO 100 $\times$  oil objective (NA: 1.40).

signal displayed punctate pattern that mainly concentrated in a small, eccentric perinuclear zone, which was similar as Mito-Tracker Deep Red-labeled signal. The overlay image of **S3** and Mito-Tracker Deep Red showed convincing yellow fluorescence in punctate pattern (Figure 7b). In contrast, the merged fluorescence signal demonstrated less coincidental staining of the ER with **S3** and ER-tracker Blue-White DPX. The overlay image of **S3**, Mito-Tracker Deep Red, and ER-tracker Blue-White DPX also implies the co-localization of the VDPs with mitochondria (Figure 7b), which was explained in detail in our previous report.<sup>[12]</sup>

Moreover, enlarged fluorescent images of **S1**-labeled cells exhibited a clear fluorescence signal (Figure 8), which needs to be further studied through proteomic analysis by using confocal microscopy and SDS-PAGE analysis. Taken together, these results suggest that **S1**, **S2**, and **S3** are highly selective fluorescent probes for VDPs and can realize the in situ imaging of VDPs in living cells. Subsequent studies will focus on further investigation of these fluorescence probes for the selective labeling of various vicinal thiols in VDPs

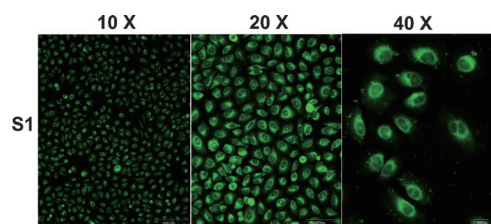


Figure 8. In-situ-imaging of VDPs in Chang liver cells with **S1** (5  $\mu\text{M}$ ). Images were taken with an Olympus IX71 microscope at 10 $\times$ , 20 $\times$  and 40 $\times$  magnification, respectively. Scale bar: 100, 50, 10  $\mu\text{m}$ , respectively.

according to the features of the probes (such as the fluorescence response of the probes at different pH values, different  $\log P$  values, and electrostatic potentials, etc.) in living cells. Meanwhile, these probes afford convenient tools for the ongoing proteomics study of various disease-related VDPs.

## Conclusion

In summary, we have expanded the conjugation approaches to afford a series of chemical probes through attachment of various functional tags (naphthalimide, NBD, fluorescein, and biotin) to different linkers (6-aminocaproic acid, succinic acid and piperazine) attached to **VTA2**. These different linkers were introduced to make the synthesis more facile. Most importantly, the property of the probes (such as  $\log P$  value, rigidity and biocompatibility, etc.) can be tuned through these linkers. Additionally, the different characteristics of the fluorophores (different pH response, hydrophobicity, etc.) make the probes suitable for potential labeling of a variety of vicinal dithiols in VDPs. These new probes will be utilized to label various types of VDPs in different microenvironments in living cells and to identify new endogenous VDPs in subsequent proteomics analyses. Especially, the fluorescence characteristics of probes **S1** and **S2** may make in situ imaging of vicinal thiols existing in different regions of VDPs in living cells possible through direct fluorescence readout. This versatile chemical strategy provides an alternative to antibody-based methods and affords a rapid, effective and convenient tool for the in situ imaging of VDPs and the ongoing proteomics study of various disease-related VDPs.

## Experimental Section

**Materials and apparatus:** All chemical reagents and solvents were purchased from Sigma–Aldrich and were used without further purification except for THF and *N,N*-dimethylformamide (DMF), which were purified according to the literature.<sup>[26]</sup> Thin-layer chromatography (TLC) was performed on silica gel plates. Column chromatography was performed by using silica gel (Hailang, Qingdao) 200–300 mesh.  $^1\text{H}$  and  $^{13}\text{C}$  NMR spectra were recorded employing a Bruker AV-400 spectrometer with chemical shifts expressed in parts per million ( $\text{Me}_4\text{Si}$  as internal standard). Electrospray ionization (ESI) mass spectrometry was performed in

a HP 1100 LC-MS spectrometer. Melting points were determined by an X-6 micro-melting point apparatus and were uncorrected. IR spectra were recorded on a Nicolet Nexus 770 spectrometer. All pH measurements were performed by using a Sartorius basic pH-Meter PB-20. Fluorescence spectra were determined using a Varian Cary Eclipse fluorescence spectrometer. Absorption spectra were determined by a Varian Cary 100 UV/Vis spectrophotometer.

**Synthesis of target probes:** The detailed syntheses of **VTA2**, **VTA4**, **VTA6**, **F2**, and other related compounds are described in the Supporting Information according to published procedures.<sup>[12]</sup>

***N*-[4-(1,3,2-Dithiarsolan-2-yl)phenyl]-6-[(7-nitrobenzo[c][1,2,5]oxadiazol-4-yl)amino]hexanamide (S1):**  $\text{Et}_3\text{N}$  (55  $\mu\text{L}$ , 0.393 mmol) was added to a solution of **VTA4** (122 mg, 0.328 mmol) in dry dichloromethane, followed by addition of 4-chloro-7-nitrobenzo[c][1,2,5]-oxadiazole (NBD-Cl, 78 mg, 0.393 mmol) in dry dichloromethane (or another procedure was that **VTA4** was dissolved in dry acetonitrile, added to potassium carbonate, then NBD-Cl in dry acetonitrile was added dropwise to the reaction mixture) at room temperature under an Ar atmosphere overnight. TLC showed that the reaction was complete, and then the solvent was removed under reduced pressure. The crude product was purified by chromatography on a silica gel column ( $\text{CH}_2\text{Cl}_2/\text{methanol}$ , 25:1, v/v) to give **S1** as a brown powder (58 mg, 33% yield). **S1** was also can be prepared through the conjugation of NBD derivative **N1** with **VTA2** in a relatively high yield (detailed procedures was described in the Supporting Information).  $^1\text{H}$  NMR (400 MHz,  $\text{CDCl}_3$ ):  $\delta$  = 8.50 (d,  $J$  = 8.8 Hz, 1H), 7.63 (d,  $J$  = 8.0 Hz, 2H), 7.54 (d,  $J$  = 8.0 Hz, 2H), 7.21 (s, 1H), 6.43 (br, 1H), 6.20 (d,  $J$  = 8.8 Hz, 1H), 3.56 (q,  $J$  = 6.4 Hz, 2H), 3.41–3.35 (m, 2H), 3.22–3.15 (m, 2H), 2.46 (t,  $J$  = 7.2 Hz, 2H), 1.93–1.82 (m, 4H), 1.64–1.56 ppm (m, 2H);  $^{13}\text{C}$  NMR (100 MHz,  $\text{CDCl}_3$ ):  $\delta$  = 170.7, 144.2, 143.9, 139.0, 138.5, 136.4, 131.6, 123.9, 119.4, 98.5, 43.5, 41.8, 37.0, 28.0, 26.2, 24.3 ppm; IR (KBr):  $\tilde{\nu}$  = 3334, 3269, 2940, 1667, 1596, 1513, 1294, 1246, 1181  $\text{cm}^{-1}$ ; HRMS (ES+):  $m/z$  calcd for  $\text{C}_{20}\text{H}_{22}\text{N}_5\text{O}_4\text{NaS}_2\text{As}$ : 558.0227 [ $M^+$ +Na]; found: 558.0222.

**Alternative approach for the synthesis of S1:** HATU (76 mg, 0.2 mmol), **VTA2** (51 mg, 0.2 mmol) and DIPEA (35  $\mu\text{L}$ , 0.2 mmol) were added to a solution of **N1** (58 mg, 0.2 mmol) in anhydrous DMF (10 mL). The mixture was stirred at room temperature for about 12 h until TLC showed that the reaction was complete. The crude product was obtained after the solvent was removed under reduced pressure and then it was purified by chromatography on a silica gel column ( $\text{CH}_2\text{Cl}_2$ : methanol, 25:1, v/v) to afford brown powder (70 mg, 65% yield).  $^1\text{H}$  NMR (400 MHz,  $\text{CDCl}_3$ ):  $\delta$  = 8.50 (d,  $J$  = 8.8 Hz, 1H), 7.63 (d,  $J$  = 8.0 Hz, 2H), 7.54 (d,  $J$  = 8.0 Hz, 2H), 7.21 (s, 1H), 6.43 (br, 1H), 6.20 (d,  $J$  = 8.8 Hz, 1H), 3.56 (q,  $J$  = 6.4 Hz, 2H), 3.41–3.35 (m, 2H), 3.22–3.15 (m, 2H), 2.46 (t,  $J$  = 7.2 Hz, 2H), 1.93–1.82 (m, 4H), 1.64–1.56 (m, 2H);  $^{13}\text{C}$  NMR (100 MHz,  $\text{CDCl}_3$ ):  $\delta$  = 170.7, 144.2, 143.9, 139.0, 138.5, 136.4, 131.6, 123.9, 119.4, 98.5, 43.5, 41.8, 37.0, 28.0, 26.2, 24.3 ppm; IR (KBr): 3334, 3269, 2940, 1667, 1596, 1513, 1294, 1246, 1181  $\text{cm}^{-1}$ ; HRMS (ES+):  $m/z$  calcd for  $\text{C}_{20}\text{H}_{22}\text{N}_5\text{O}_4\text{NaS}_2\text{As}$ : 558.0227 [ $M^+$ +Na]; found: 558.0222.

**6-[(7-Nitrobenzo[c][1,2,5]oxadiazol-4-yl)amino]-*N*-phenylhexanamide (SC1):** Compound **SC1** was prepared by the reaction of **VTAC2** with 4-chloro-7-nitrobenzo[c][1,2,5]-oxadiazole (NBD-Cl) to give a dark red solid (0.23 g, 88% yield). The procedure was the similar as synthesis of **S1**.  $^1\text{H}$  NMR (400 MHz,  $[\text{D}_6]\text{DMSO}$ ):  $\delta$  = 9.85 (s, 1H), 9.58 (br, 1H), 8.49 (d,  $J$  = 8.8 Hz, 2H), 7.55 (d,  $J$  = 7.6 Hz, 2H), 7.28–7.24 (m, 2H), 7.02–6.98 (m, 1H), 6.41 (d,  $J$  = 7.2 Hz, 1H), 3.49–3.46 (m, 2H), 2.31 (t,  $J$  = 7.2 Hz, 2H), 1.75–1.60 (m, 4H), 1.45–1.37 ppm (m, 2H);  $^{13}\text{C}$  NMR (100 MHz,  $[\text{D}_6]\text{DMSO}$ ):  $\delta$  = 171.5, 139.7, 138.4, 134.9, 129.0, 123.3, 119.4, 111.1, 99.6, 43.6, 36.7, 27.9, 26.5, 25.2 ppm; MS (ESI):  $m/z$  (%): 370 (100) [ $M^+$ +H].

***N*-[4-(1,3,2-Dithiarsolan-2-yl)phenyl]-5-[(3*a*,4*S*,6*a**R*)-2-oxohexahydro-1*H*-thieno[3,4-*d*]imidazol-4-yl]pentanamide (S4):** 5-[(3*a*,4*S*,6*a**R*)-2-Oxohexahydro-1*H*-thieno[3,4-*d*]imidazol-4-yl]pentanoic acid (*D*-(+)-biotin, 244 mg, 1.0 mmol) and hydroxybenzotriazole (HOBT, 27 mg, 0.2 mmol) were suspended in anhydrous DMF (10 mL), and heated until a clear solution was obtained. Then the reaction mixture was cooled to room temperature and a solution of DCC in  $\text{CH}_2\text{Cl}_2$  (2.7 mL of a 1.0 M solution in  $\text{CH}_2\text{Cl}_2$ , 2.7 mmol) was added dropwise and the mixture remained stirring at room temperature for another 3 h. **VTA2** (311 mg, 1.2 mmol) and

DMAP (12 mg, 0.1 mmol) were added, and the mixture was warmed to 60°C and it continued to stir for 4 h. Then the mixture was cooled to room temperature and it continued to stir for 24 h. TLC showed that the reaction was complete. Then, the solvent was removed under reduced pressure. The residue was dissolved in CH<sub>2</sub>Cl<sub>2</sub> (80 mL), washed with water (40 mL), ice-cold HCl solution (5%, 40 mL), and saturated NaHCO<sub>3</sub> (40 mL × 2), brine (40 mL). The organic layer was taken to dryness under reduced pressure. The crude product was purified by chromatography on a silica gel column (petroleum ether: EtOAc, 2:1, v/v) to give **S4** as a white powder (350 mg, 72% yield). <sup>1</sup>H NMR (400 MHz, [D<sub>6</sub>]DMSO): δ = 9.97 (s, 1H), 7.61 (d, *J* = 8.4 Hz, 2H), 7.55 (d, *J* = 8.4 Hz, 2H), 6.42 (s, 1H), 6.35 (s, 1H), 4.32–4.29 (m, 1H), 4.14–4.12 (m, 1H), 3.38–3.32 (m, 2H), 3.19–3.09 (m, 3H), 2.82 (dd, *J*<sub>1</sub> = 12.4 Hz and *J*<sub>2</sub> = 5.2 Hz, 1H), 2.57 (d, *J* = 12.4 Hz, 1H), 2.30 (t, *J* = 7.2 Hz, 2H), 1.64–1.58 (m, 4H), 1.52–1.45 (m, 1H), 1.42–1.33 ppm (m, 2H); <sup>13</sup>C NMR (100 MHz, [D<sub>6</sub>]DMSO): δ = 171.8, 163.1, 140.6, 137.3, 131.7, 119.2, 61.5, 59.6, 55.8, 41.8, 36.6, 28.6, 28.5, 25.5 ppm; IR (KBr):  $\tilde{\nu}$  = 3334, 3269, 1657, 1596, 1513, 1294, 1246, 1181 cm<sup>-1</sup>; HRMS (ES+): *m/z* calcd for C<sub>18</sub>H<sub>24</sub>N<sub>3</sub>O<sub>2</sub>NaS<sub>3</sub>As: 508.0114 [*M*<sup>+</sup>+Na]; found: 508.0145.

**N-[4-(1,3,2-Dithiansolan-2-yl)phenyl]-4-[4-[2-(6-hydroxy-3-oxo-3H-xanthen-9-yl)benzoyl]piperazin-1-yl]-4-oxobutanamide (S2)**: HATU (76 mg, 0.2 mmol), VTA6 (72 mg, 0.2 mmol), and DIPEA (35 μL, 0.2 mmol) were added to a solution of **F2** (80 mg, 0.2 mmol) in anhydrous DMF (10 mL). The mixture was stirred at room temperature for about 12 h until TLC showed that the reaction was complete. The crude product was obtained after the solvent was removed under reduced pressure. Then, the crude material was purified by chromatography on a silica gel column (CH<sub>2</sub>Cl<sub>2</sub>/methanol, 20:1, v/v) to afford a red solid (46 mg, 31% yield). <sup>1</sup>H NMR (400 MHz, [D<sub>6</sub>]DMSO): δ = 10.25 (brs, 1H), 7.61 (br, 6H), 7.55–7.53 (m, 3H), 7.39 (s, 1H), 8.61 (d, *J* = 6.8 Hz, 2H), 6.09 (d, *J* = 8.0 Hz, 2H), 5.99 (s, 1H), 3.28–3.15 (m, 12H), 2.56–2.54 (m, 2H), 2.03–1.97 ppm (m, 2H); <sup>13</sup>C NMR (100 MHz, [D<sub>6</sub>]DMSO): δ = 157.6, 148.5, 140.8, 137.1, 135.9, 132.6, 131.7, 130.8, 130.4, 130.3, 129.6, 129.1, 123.5, 119.0, 103.5, 44.9, 41.7, 31.7, 29.5, 29.2, 22.5 ppm; HRMS (ES+): *m/z* calcd for C<sub>36</sub>H<sub>34</sub>N<sub>3</sub>O<sub>6</sub>NaS<sub>2</sub>As: 765.0880 [*M*<sup>+</sup>+Na]; found 765.0890.

**4-[4-[2-(6-Hydroxy-3-oxo-3H-xanthen-9-yl)benzoyl]piperazin-1-yl]-4-oxo-N-phenylbutanamide (SC2)**: **SC2** was prepared by reaction of **VTAC6** with **F2** to give a yellow solid (26 mg, 74% yield). The procedure was the similar as synthesis of **S2**. <sup>1</sup>H NMR (400 MHz, CD<sub>3</sub>OD): δ = 7.76 (brs, 2H), 7.68–7.67 (m, 2H), 7.53 (d, *J* = 6.8 Hz, 3H), 7.30 (t, *J* = 8.0 Hz, 2H), 7.21 (d, *J* = 8.8 Hz, 2H), 7.08 (t, *J* = 7.2 Hz, 2H), 6.75–6.73 (m, 4H), 3.48–3.39 (m, 8H), 2.69–2.68 ppm (m, 2H); <sup>13</sup>C NMR (100 MHz, CD<sub>3</sub>OD): δ = 158.2, 149.5, 141.4, 137.1, 135.2, 132.6, 131.7, 131.4, 131.0, 130.8, 129.6, 128.3, 123.6, 119.7, 104.1, 44.9, 41.7, 31.7, 27.4 ppm; MS (ESI): *m/z* (%): 576 (100) [*M*<sup>+</sup>–H].

**SDS-PAGE and fluorescence imaging of gels**: The selectivity of probes was verified by 15% SDS-PAGE. Samples were labeled in the PBS buffer at 37°C for 30 min, with a final concentration of protein at 10 μM, the probes at 50 μM. After labeling, the samples were mixed with SDS-PAGE loading buffer without β-mercaptoethanol, and the electrophoresis was performed immediately. The gel was imaged by Carestream in vivo imaging FX System (excitation: 460 nm, emission: 535 nm for **S1/S2**). The same gel was also stained by Coomassie brilliant blue (CBB) after the fluorescent image was obtained.

**Cell culture**: Chang liver cells were obtained from American Type Culture collection. Chang liver cells were grown in Dulbecco's modified Eagle's medium (DMEM, high glucose medium) supplemented with 10% fetal bovine serum (FBS) and typically passaged with sub-cultivation ratio of 1:4 every two days. Cells were incubated in a 5% CO<sub>2</sub> humidified incubator at 37°C.

**MTT assay**: Chang liver cells were seeded to Corning 96 well plate the day before detection with about 80% intensity. During detection, cells were treated with different concentration of **S1** and **S2**, respectively, and then the cell viability was tested by using the CellTiter 96 AQueous non-radioactive cell proliferation assay kit (Promega).

**Cell labeling and in situ imaging**: The Chang liver cells seeded to 35 mm glass bottom dishes the day before imaging to get the cell density about 80%. The cells were labeled with 5 μM of **S1/SC1/S2/SC2/S3/SC3** in

DPBS (containing 1% DMSO, v/v) at 37°C. After 30 min for **S1/SC1**, **S2**, **SC2**, **S3**, and **SC3**, respectively, the cells were washed three times to remove unbound probes before in situ imaging with a fluorescence microscope (Olympus IX71, magnification 10×, 20× and 40×) with excitation by 488 nm laser, and 500–550 nm emission light was collected for **S1**, **SC1**, **S2**, **SC2**, **S3**, and **SC3**.

**Co-localization of S3 with ER-tracker and Mito-tracker**: For triple-staining of ER, mitochondria, and **S3**, the cells were first labeled by using Mito-tracker Deep Red (50 nm), then **S3** (5 μM) in DPBS with 1% DMSO for 30 min at 37°C, then finally ER-tracker Blue-White DPX (100 nm). To exclude the interference to the fluorescent signal, the following emission/excitation wavelengths were used: excitation of ER-tracker Blue-White DPX at 405 nm, 425–490 nm emission light was collected. Excitation of **S3** at 488 nm, 500–600 nm emission light was collected. Excitation of Mito-Tracker Deep red 635 nm, >650 nm emission light was collected.

## Acknowledgements

We thank the financial support from National Natural Science Foundation of China (Grants 21076077, 21236002), the National Basic Research Program of China (973 Program, 2013CB733700, 2010CB126100), the National High Technology Research and Development Program of China (863 Program, 2011AA10A207), Shanghai Pujiang Program and the Fundamental Research Funds for the Central Universities, The Innovative Program of Shanghai Normal University (SK201331), the Science and Technology Innovation Foundation for College Students (B-7062-12-001114).

- [1] a) B. A. Maron, S. S. Tang, J. Loscalzo, *Antioxid. Redox Signaling* **2013**, *18*, 270–287; b) I. Pe'er, C. E. Felder, O. Man, I. Silman, J. L. Sussman, J. S. Beckmann, *Proteins Struct. Funct. Bioinf.* **2004**, *54*, 20–40; c) J. Ying, N. Clavreul, M. Sethuraman, T. Adachi, R. A. Cohen, *Free Radical Biol. Med.* **2007**, *43*, 1099–1108; d) K. G. Reddie, K. S. Carroll, *Curr. Opin. Chem. Biol.* **2008**, *12*, 746–754; e) L. B. Poole, K. J. Nelson, *Curr. Opin. Chem. Biol.* **2008**, *12*, 18–24; f) B. A. Maron, J. Loscalzo, *Clin. Lab. Med.* **2006**, *26*, 591–609.
- [2] a) M. Valko, C. J. Rhodes, J. Moncol, M. Izakovic, M. Mazur, *Chem.-Biol. Interact.* **2006**, *160*, 1–40; b) X. W. Zhang, X. J. Yan, Z. R. Zhou, F. F. Yang, Z. Y. Wu, H. B. Sun, W. X. Liang, A. X. Song, V. Lallemand-Breitenbach, M. Jeanne, Q. Y. Zhang, H. Y. Yang, Q. H. Huang, G. B. Zhou, J. H. Tong, Y. Zhang, J. H. Wu, H. Y. Hu, H. de The, S. J. Chen, Z. Chen, *Science* **2010**, *328*, 240–243.
- [3] N. Houstis, E. D. Rosen, E. S. Lander, *Nature* **2006**, *440*, 944–948.
- [4] a) L. J. Matthias, P. J. Hogg, *Antioxid. Redox Signaling* **2003**, *5*, 133–138; b) B. Sahaf, K. Heydari, L. A. Herzenberg, L. A. Herzenberg, *Arch. Biochem. Biophys.* **2005**, *434*, 26–32; c) W. Ou, J. Silver, *Virology* **2006**, *350*, 406–417.
- [5] G. Bánhegyi, J. Mandl, M. Csala, *J. Neurochem.* **2008**, *107*, 20–34.
- [6] A. Bachi, I. Dalle-Donne, A. Scaloni, *Chem. Rev.* **2013**, *113*, 596–698.
- [7] R. Requejo, E. T. Chouchani, A. M. James, T. A. Prime, K. S. Lilley, I. M. Fearley, M. P. Murphy, *Arch. Biochem. Biophys.* **2010**, *504*, 228–235.
- [8] a) C. Gitler, B. Zarmi, E. Kalef, *Anal. Biochem.* **1997**, *252*, 48–55; b) G. P. McStay, S. J. Clarke, A. P. Halestrap, *Biochem. J.* **2002**, *367*, 541–548; c) R. D. Hoffman, M. D. Lane, *J. Biol. Chem.* **1992**, *267*, 14005–14011.
- [9] a) J. Heredia-Moya, K. L. Kirk, *Bioorg. Med. Chem.* **2008**, *16*, 5743–5746; b) R. Moaddel, A. Sharma, T. Huseni, G. S. Jones, R. N. Hanson, R. H. Loring, *Bioconjugate Chem.* **1999**, *10*, 629–637.
- [10] S. Girouard, M. H. Houle, A. Grandbois, J. W. Keillor, S. W. Michnick, *J. Am. Chem. Soc.* **2005**, *127*, 559–566.

- [11] a) N. Donoghue, P. T. Yam, X. M. Jiang, P. J. Hogg, *Protein Sci.* **2000**, *9*, 2436–2445; b) X. Zhang, F. Yang, J. Y. Shim, K. L. Kirk, D. E. Anderson, X. Chen, *Cancer Lett.* **2007**, *255*, 95–106.
- [12] C. Huang, Q. Yin, W. Zhu, Y. Yang, X. Wang, X. Qian, Y. Xu, *Angew. Chem.* **2011**, *123*, 7693–7698; *Angew. Chem. Int. Ed.* **2011**, *50*, 7551–7556.
- [13] a) L. I. Leichert, U. Jakob, *Antioxid. Redox Signaling* **2006**, *8*, 763–772; b) R. L. Krauth-Siegel, H. Bauer, R. H. Schirmer, *Angew. Chem.* **2005**, *117*, 698–724; *Angew. Chem. Int. Ed.* **2005**, *44*, 690–715.
- [14] a) P. Eaton, *Free Radical Biol. Med.* **2006**, *40*, 1889–1899; b) J. E. Biaglow, I. S. Ayene, S. W. Tuttle, C. J. Koch, J. Donahue, J. J. Mieyal, *Radiat. Res.* **2006**, *165*, 307–317.
- [15] E. Adams, D. Jeter, A. W. Cordes, J. W. Kolis, *Inorg. Chem.* **1990**, *29*, 1500–1503.
- [16] W. L. Zahler, W. W. Cleland, *J. Biol. Chem.* **1968**, *243*, 716–719.
- [17] F. Knoch, T. Schmachtel, V. Ullrich, *Z. Kristallogr.* **1995**, *210*, 642–642.
- [18] a) N. Wimmer, J. A. Robinson, N. Gopisetty-Venkatta, S. J. Roberts-Thomson, G. R. Monteith, I. Toth, *Med. Chem.* **2006**, *2*, 79–87; b) M. L. Carbajal, S. L. S. Espinoza, S. N. Valdez, E. Poskus, E. E. Smolko, M. Grasselli, *React. Funct. Polym.* **2009**, *69*, 816–820.
- [19] a) B. A. Griffin, S. R. Adams, R. Y. Tsien, *Science* **1998**, *281*, 269–272; b) S. R. Adams, R. E. Campbell, L. A. Gross, B. R. Martin, G. K. Walkup, Y. Yao, J. Llopis, R. Y. Tsien, *J. Am. Chem. Soc.* **2002**, *124*, 6063–6076.
- [20] a) G. J. Mercer, M. S. Sigman, *Org. Lett.* **2003**, *5*, 1591–1594; b) Y. Niu, H. Hou, Y. Wei, Y. Fan, Y. Zhu, C. Du, X. Xin, *Inorg. Chem. Commun.* **2001**, *4*, 358–361.
- [21] a) P. Workman, I. Collins, *Chem. Biol.* **2010**, *17*, 561–577; b) S. V. Frye, *Nat. Chem. Biol.* **2010**, *6*, 159–161.
- [22] a) K. Chen, Y. Lin, T. Detwiler, *Blood* **1992**, *79*, 2226–2228; b) D. Essex, K. Chen, M. Swiatkowska, *Blood* **1995**, *86*, 2168–2173; c) H. Kutsumi, K. Kawai, R. J. Johnston, K. Rokutan, *Blood* **1995**, *85*, 2559–2569.
- [23] a) A. Chattopadhyay, *Chem. Phys. Lipids* **1990**, *53*, 1–15; b) S. Haldar, A. Chattopadhyay, *Fluorescent Methods to Study Biological Membranes, Vol. 13* (Eds.: Y. Mély, G. Duportail), Springer, Berlin Heidelberg, **2013**, pp. 37–50.
- [24] M. M. Altamirano, J. A. Plumbridge, M. L. Calcagno, *Biochemistry* **1992**, *31*, 1153–1158.
- [25] S. Izumi, Y. Urano, K. Hanaoka, T. Terai, T. Nagano, *J. Am. Chem. Soc.* **2009**, *131*, 10189–10200.
- [26] W. L. F. Armarego, D. D. Perrin, *Purification of Laboratory Chemicals*, 4th ed., Elsevier, Burlington, **1996**.

Received: February 13, 2013  
Published online: April 16, 2013